

Supplementary Material

# Upcycling birch bark suberin into versatile and recyclable thermosets

Fengyang Wang <sup>1</sup>, Ruslan Gryaznov <sup>1,2</sup>, Pavel Vostrejs <sup>1</sup>, Matilda Andersson <sup>1</sup>,  
Jānis Rižikovs <sup>1</sup>, Ievgen Pylypchuk <sup>1</sup>, Alberto J. Huertas-Alonso\*<sup>1</sup>, Mika H.  
Sipponen\*<sup>1,2</sup>

<sup>1</sup> Department of Chemistry, Stockholm University,  
SE-10691, Stockholm, Sweden

<sup>2</sup> Department of Chemistry, Wallenberg Wood Science Center, Stockholm  
University,  
SE-10691, Stockholm, Sweden

<sup>3</sup> Latvian State Institute of Wood Chemistry, Biorefinery Laboratory, Latvia

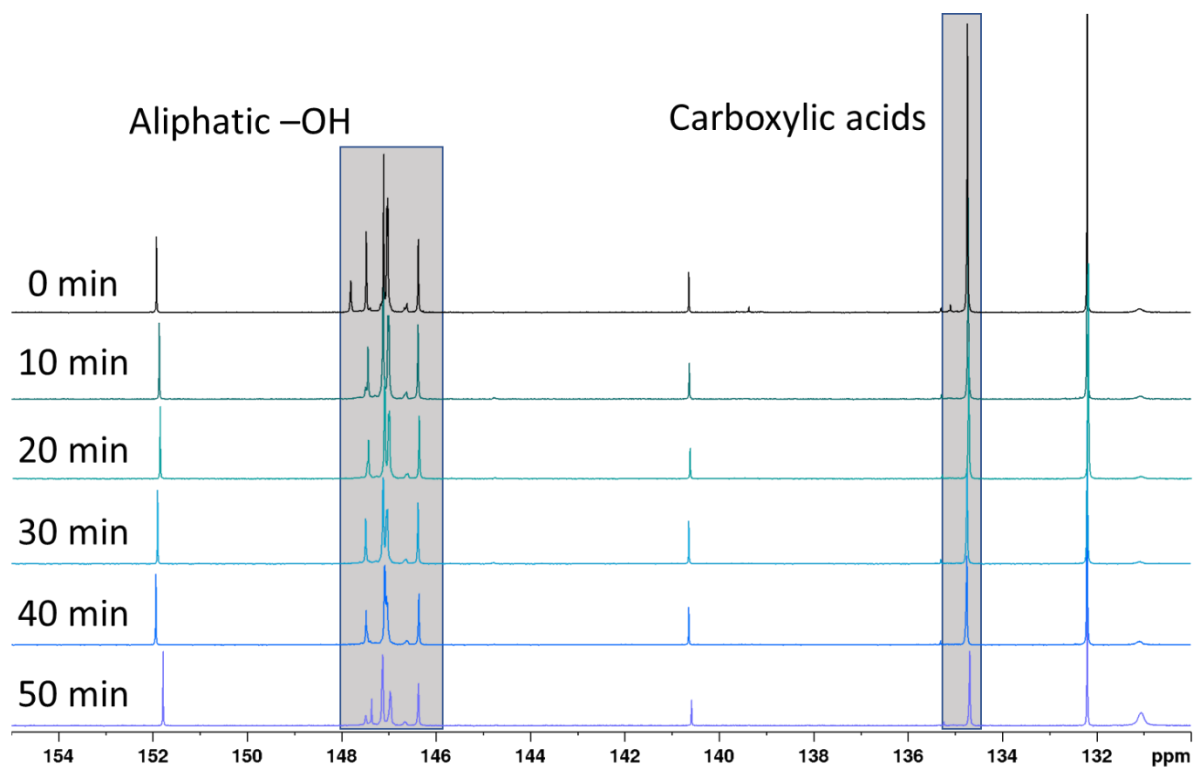
\*Corresponding to [alberto.jose.huertasalonso@su.se](mailto:alberto.jose.huertasalonso@su.se); [mika.sipponen@su.se](mailto:mika.sipponen@su.se)

Table S1 shows the detailed composition of suberinic acids used in the current study, which was modified from previously published data.

**Table. S1.** Composition of suberinic acids, modified from previously published data<sup>[1]</sup>.

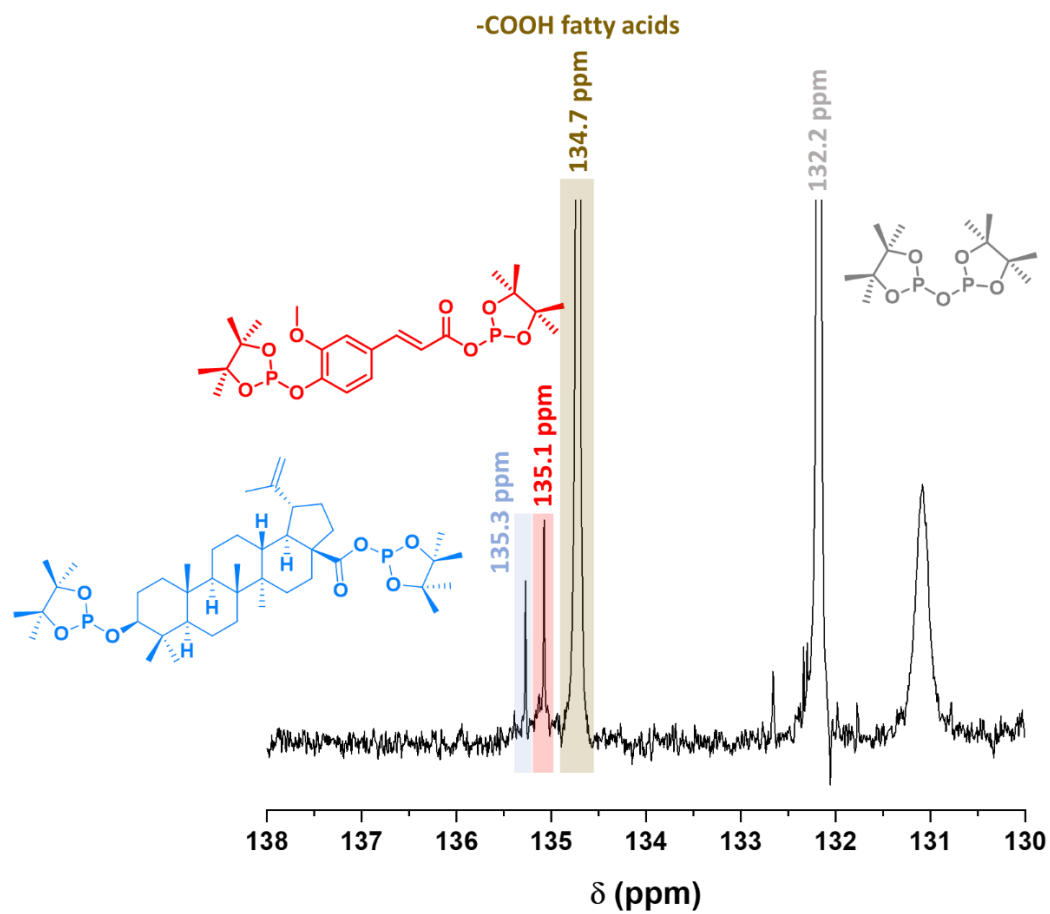
<b>Hydroxyacids</b>	<b>29.2%</b>	<b>Diacids</b>	<b>10.4%</b>
2-hydroxydecanedioic acid	21.3%	pentanedioic acid	5.4%
22-hydroxydocosanoic acid	4.7%	10,12-docosadiynedioic acid	2.4%
20-hydroxyicosanoic acid	2.6%	Hexadecanedioic acid	1.4%
3-hydroxyhexadecanoic acid	0.6%	Octanedioic acid	1.2%
<b>Extractives</b>	<b>39.5%</b>	<b>Aromatics</b>	<b>6%</b>
Betulin	36%	isoferulic acid	4.8%
Lupeol	3.5%	Oxyisoflavone	0.9%
<b>Alkanoic acid</b>	<b>12.4%</b>	Vanilic acid	0.3%
9,12-octadecadienoic acid	8.2%	<b>2-oleoylglycerol</b>	<b>0.8%</b>
Octanoic acid	4.2%	<b>Others</b>	<b>1.7%</b>

Figure S1 shows the  $^{31}\text{P}$  NMR spectra used for the quantitative analysis of hydroxyl groups in suberic acids cured for different time lengths.



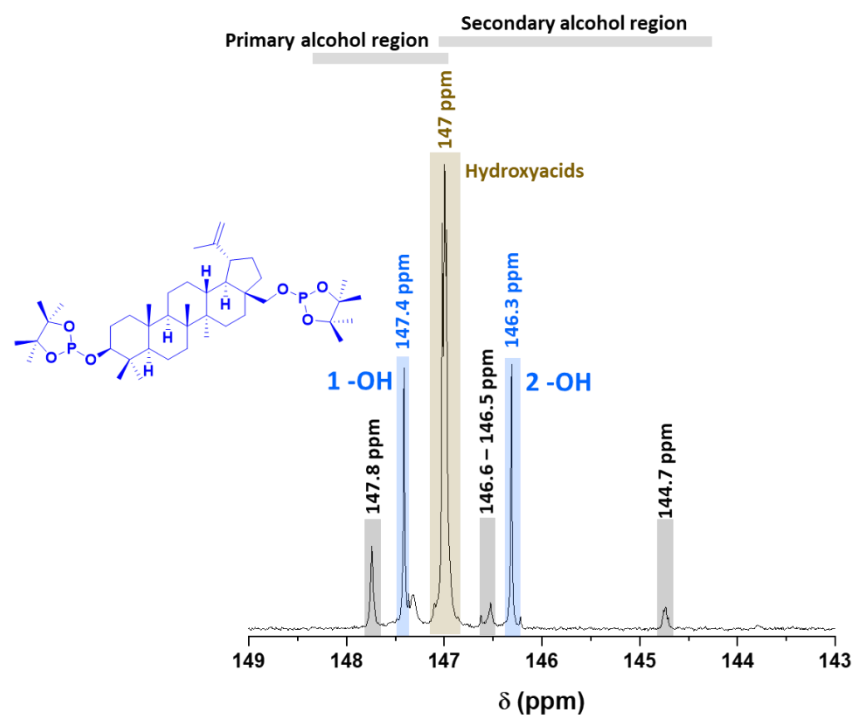
**Fig. S1.** Comparison of aliphatic -OH region and -COOH region of suberic acids in  $^{31}\text{P}$  NMR spectra from 0 to 50 minutes of thermal polymerization at 190 °C. Spectra are normalised to internal standard.

Figure S2 highlights the carboxylic acids region in the  $^{31}\text{P}$  NMR spectra of suberinic acids. The blue area indicates betulonic acid, red area refers to trans-ferulic acid, and the brown area is from aliphatic carboxylic acids.



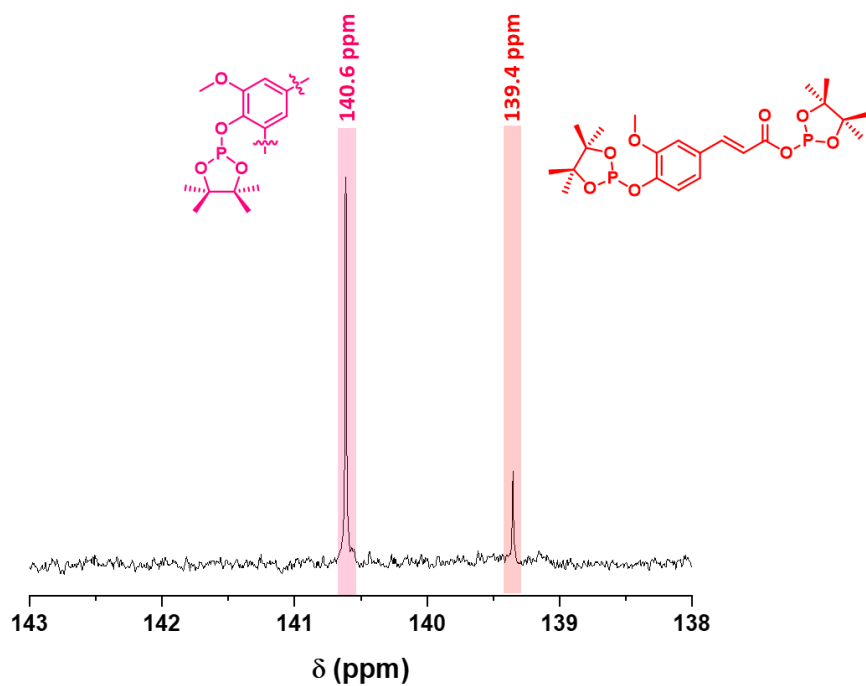
**Fig. S2.** Carboxylic acids region in the  $^{31}\text{P}$  NMR spectra of suberinic acids.

Figure S3 highlights the aliphatic -OH region in the  $^{31}\text{P}$  NMR spectra of suberinic acids. The blue area at 147 and 146 ppm represents the primary and secondary -OH of betulin, respectively. The brown area refers to the -OH from hydroxy acids.



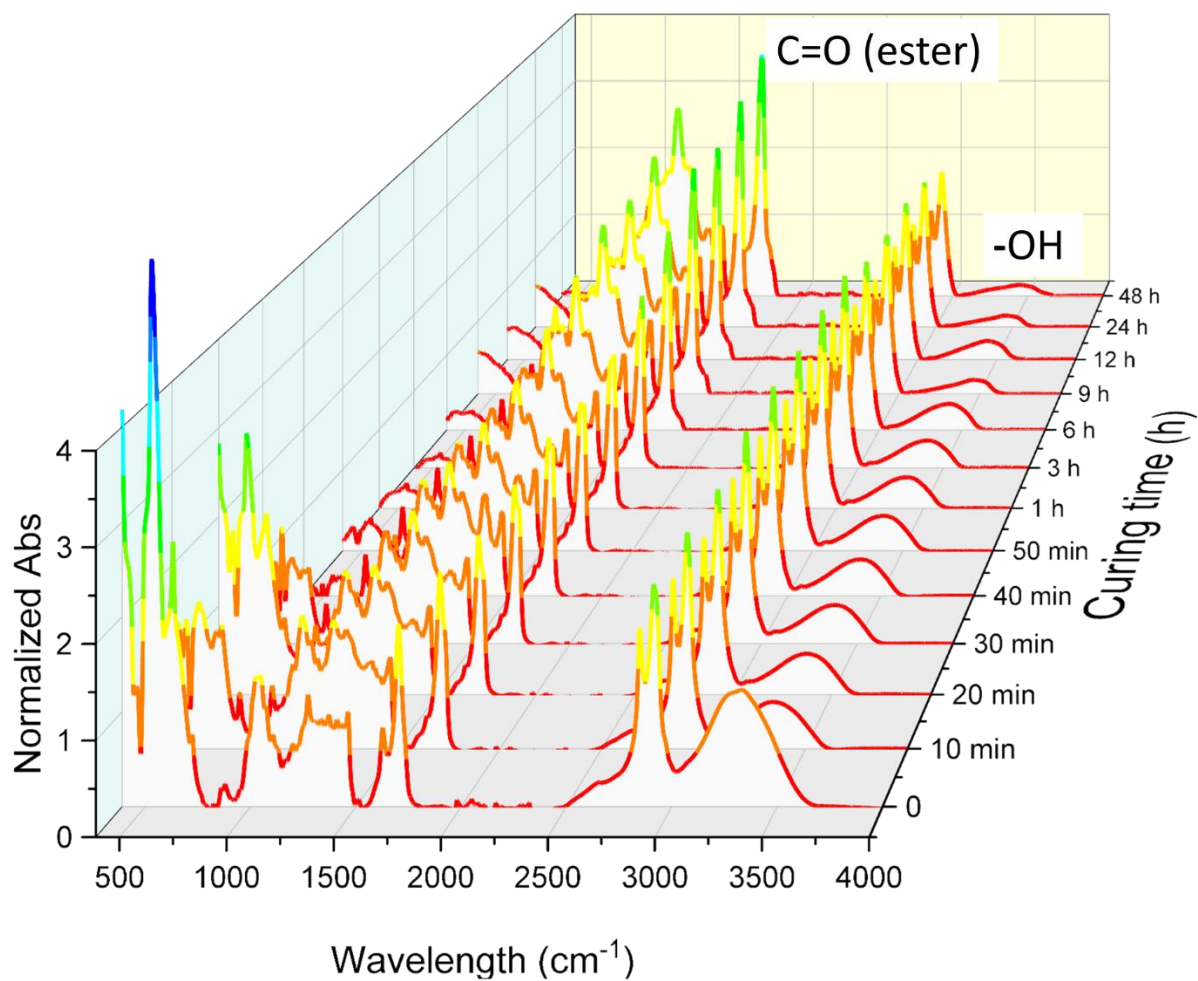
**Fig. S3.** Aliphatic -OH region in the  $^{31}\text{P}$  NMR spectra of suberinic acids.

Figure S4 highlights the aliphatic -OH region in the  $^{31}\text{P}$  NMR spectra of suberinic acids. The peaks at 140 and 139 ppm represent the secondary -OH of condensed guaiacyl and ferulic acid, respectively.



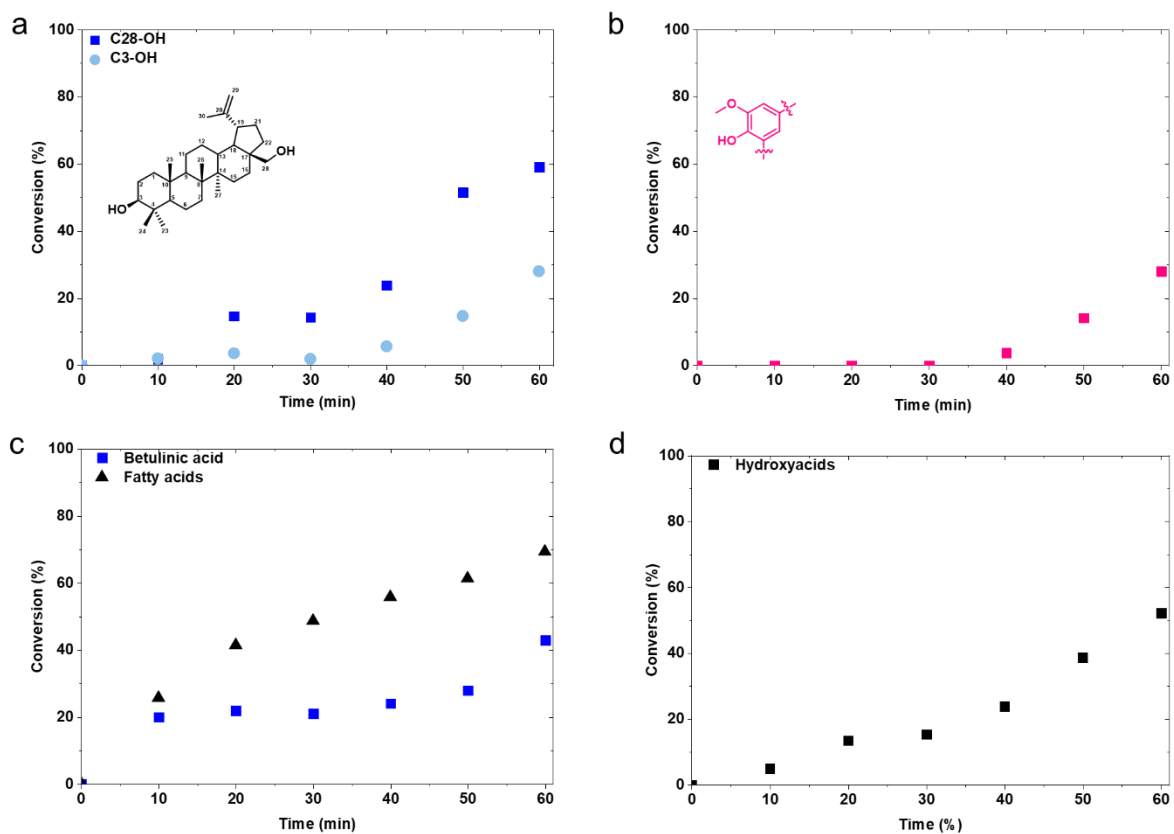
**Fig. S4.** Phenolic -OH region in the  $^{31}\text{P}$  NMR spectra of suberinic acids.

Figure S5 shows the full representative ATR-FTIR spectra of suberic acids polymerized from 0 to 48 hours at 190 °C, where intensity of -OH group drops over time and C=O (ester) peak intensity increases.



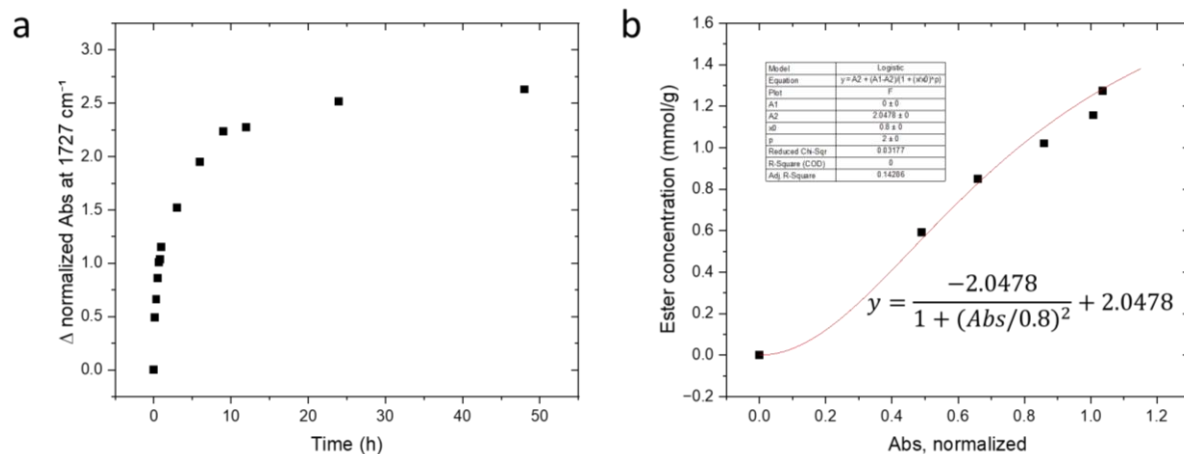
**Fig. S5.** Full representative ATR-FTIR spectra of suberic acids polymerized from 0 to 48 hours at 190 °C.

Figure S6 shows the quantitative analysis of the conversion rates of the main species in suberinic acids involved in the polycondensation reaction.



**Fig. S6.** The conversion rate of the main species in suberinic acids during the first hour of polymerization. a) Conversion rates of primary -OH and secondary -OH in betulin. b) Conversion rate of the secondary -OH from condensed guaiacyl. c) Conversion rates of -COOH from fatty acids and betulinic acid. d) Conversion rate of the -OH from hydroxyacids.

Figure S7 a) shows the change of normalized absorbance at 1727 cm<sup>-1</sup> in the IR spectra of suberinic acids polymerized from 0 to 48 hours at 190 °C. Figure S5 b) shows the correlation between the newly formed ester concentration (recalculated from <sup>31</sup>P NMR based on the decrease in carboxylic acids concentration) and normalized absorbance at 1727 cm<sup>-1</sup> in IR spectra, as well as the fitting of the correlation.



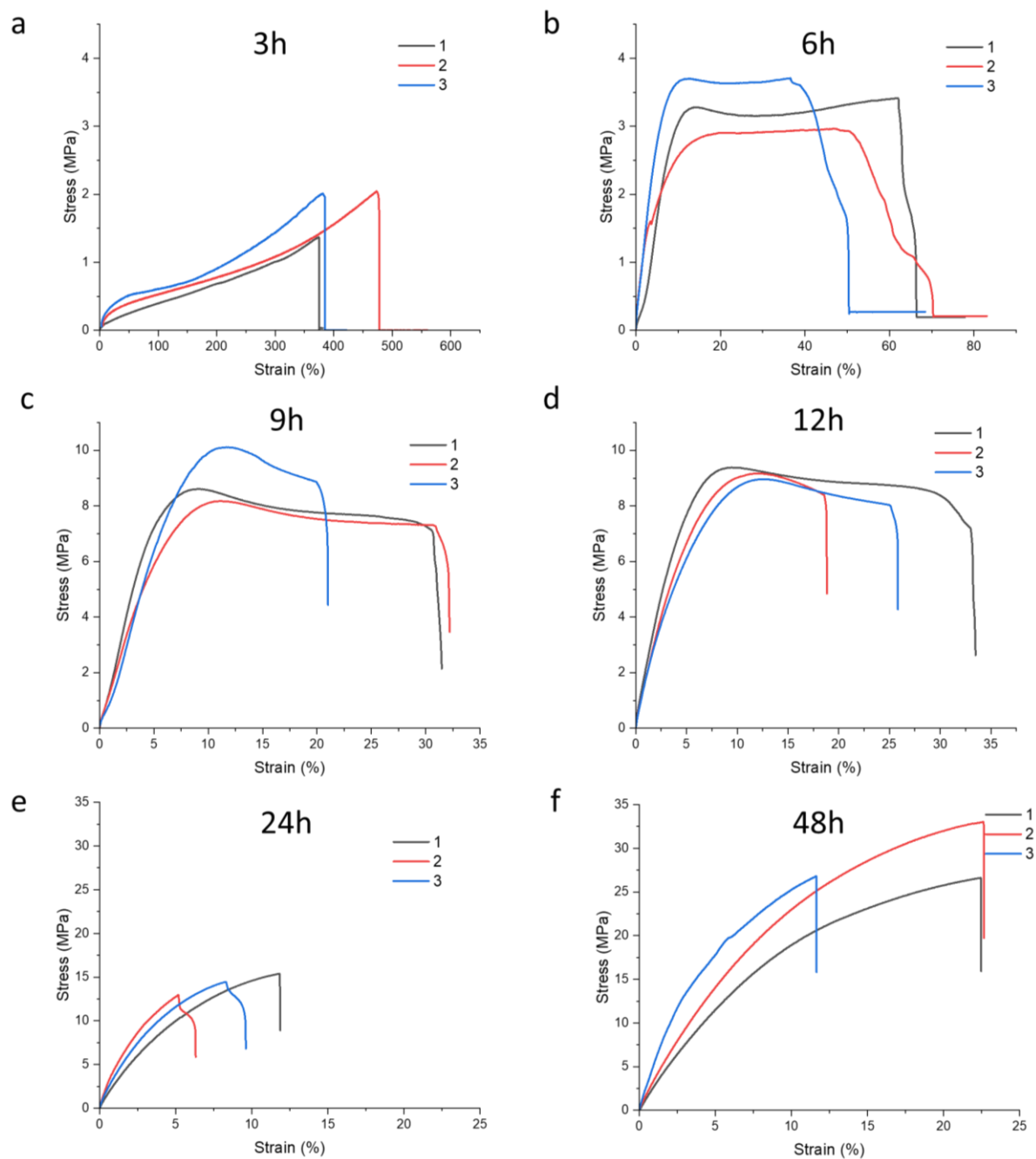
**Fig. S7.** a) Increase in the normalized absorbance at 1727 cm<sup>-1</sup> in IR spectra from 0 to 48 hours. b) Fitting of the ester concentration (measured with <sup>31</sup>P NMR) and increases in the normalized absorbance at 1727 cm<sup>-1</sup> in IR spectra.

Equation S1 shows the calculation of the average functionality of suberinic acids from the degree of reaction at gel point.

#### Equation S1

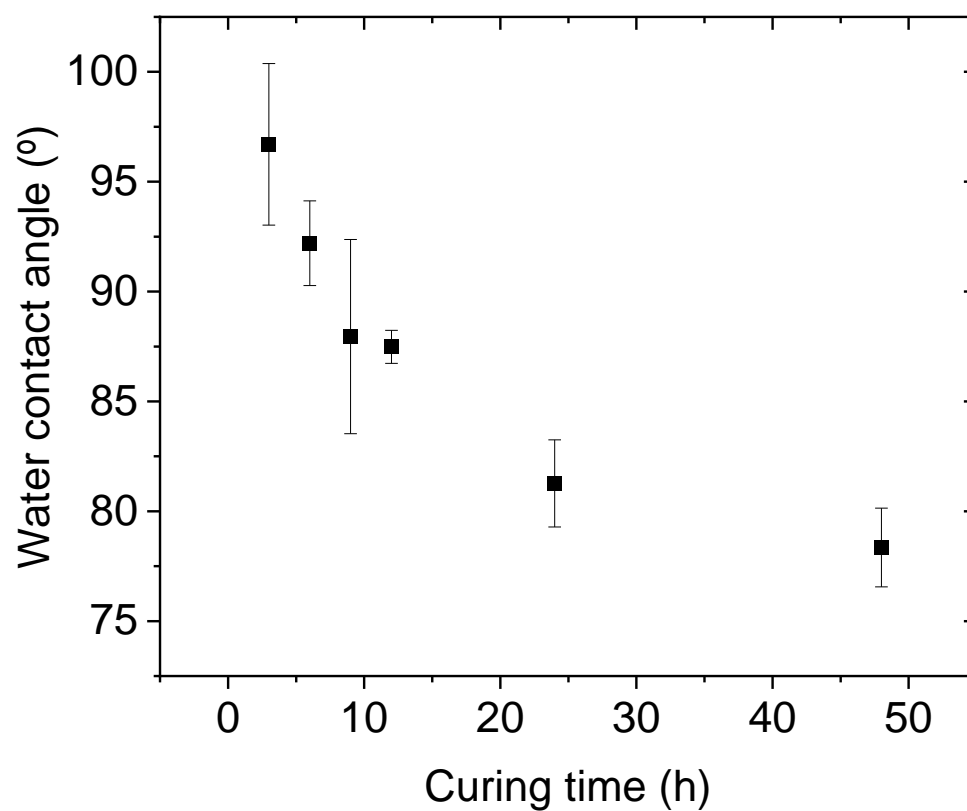
$$\text{average functionality} = 1 + \frac{1}{\text{degree of reaction at gel point}}$$

Figure S8 shows the stress-strain curves of suberinic acids thermosets polymerized at 190 °C for different time lengths (3h, 6h, 9h, 12h, 24h, 48h).



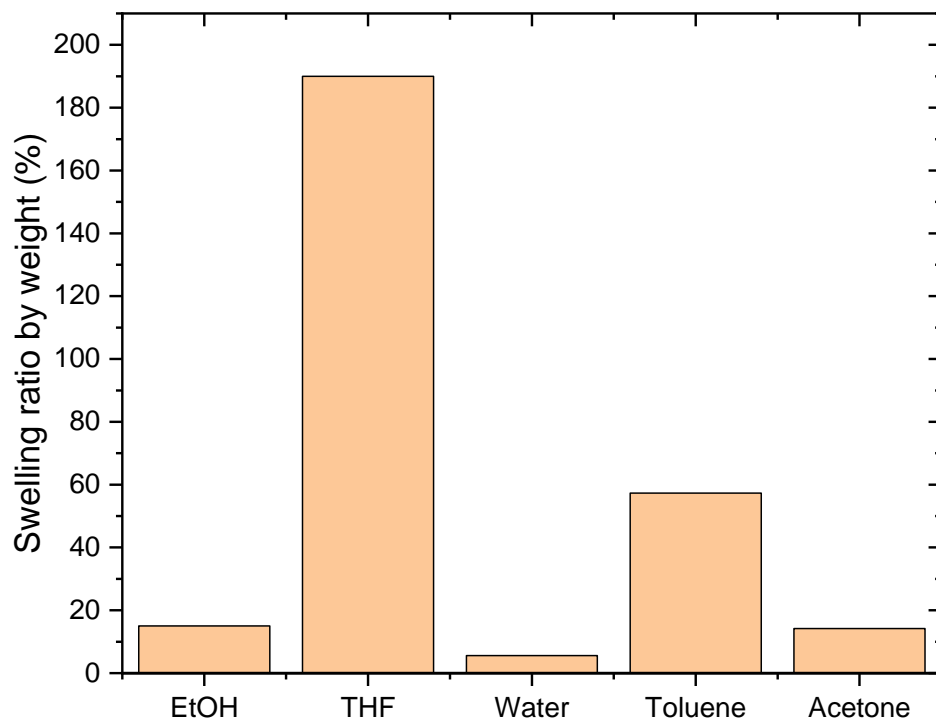
**Fig. S8.** Stress-strain curves of suberinic acids thermosets polymerized at 190 °C for different time lengths. a) 3 hours, b) 6 hours, c) 9 hours, d) 12 hours, e) 24 hours, and f) 48 hours.

Figure S9 shows the decrease in water contact angles of suberinic acids thermosets with increasing polymerization time.



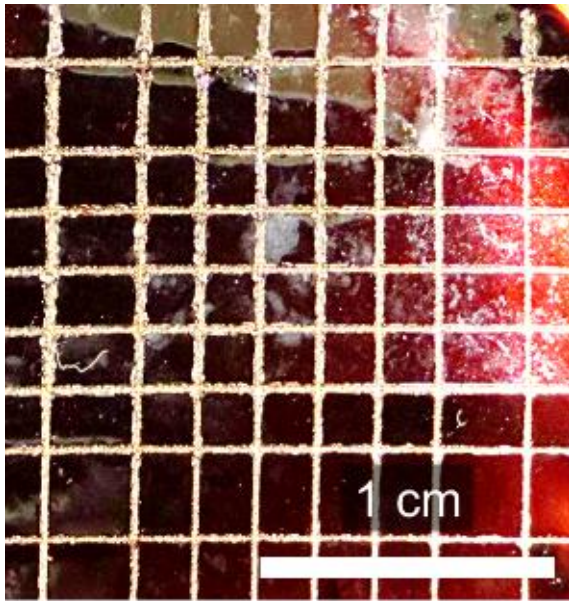
**Fig. S9.** Water contact angles of suberinic acids thermosets polymerized at 190 °C for different time lengths, 3 – 48 hours.

Figure S10 shows the weight-based swelling ratio of suberinic acids thermosets in ethanol, THF, water, toluene, and acetone.



**Fig. S10.** Swelling ratio (by weight %) of suberinic acids thermosets in ethanol, THF, water, toluene, and acetone.

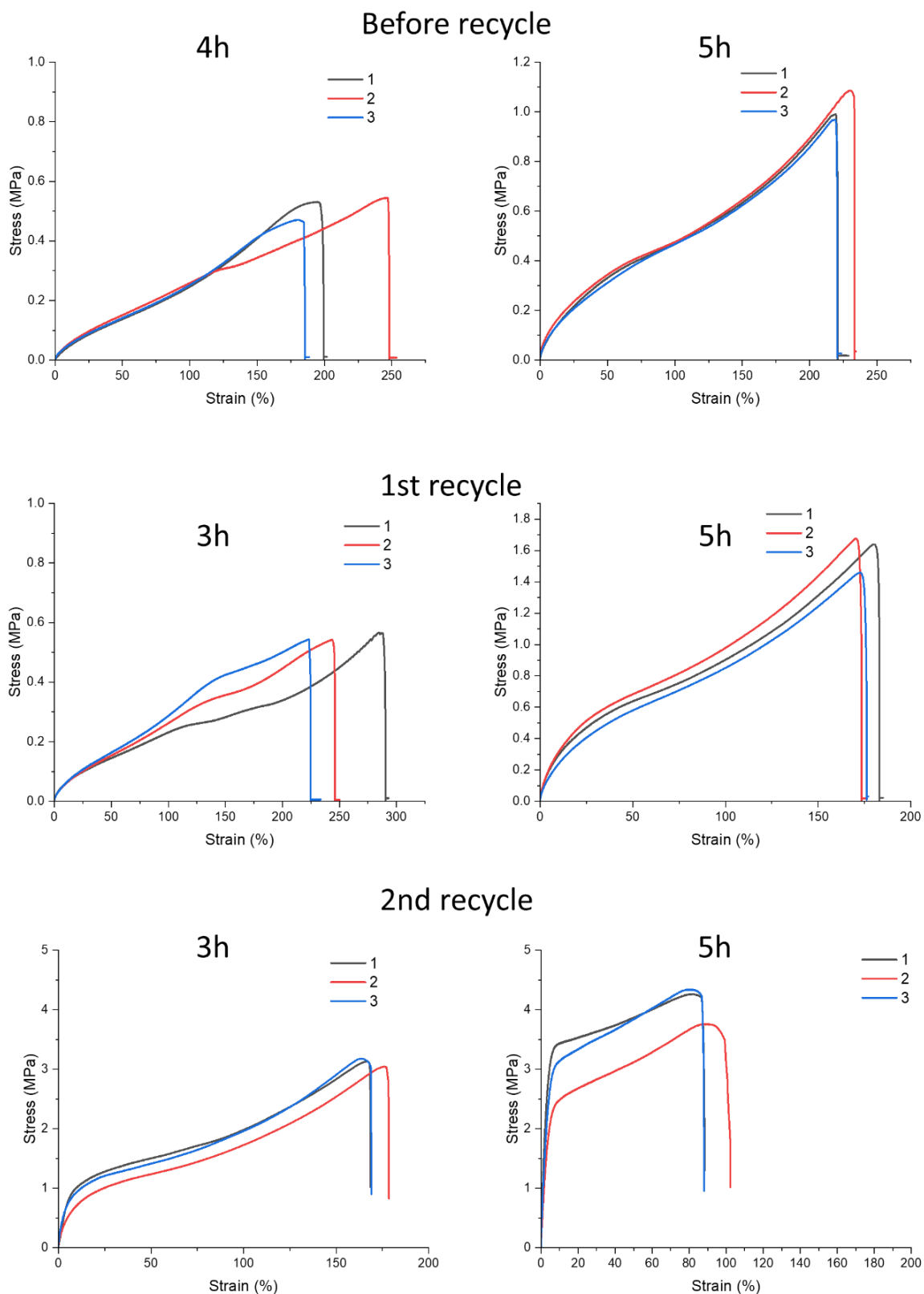
Figure S11 shows the result of the cross-cut test for examining the paint coatings' resistance to separate from substrates, where no visible coating delamination is found after the test.



Metal coating  
adhesion test

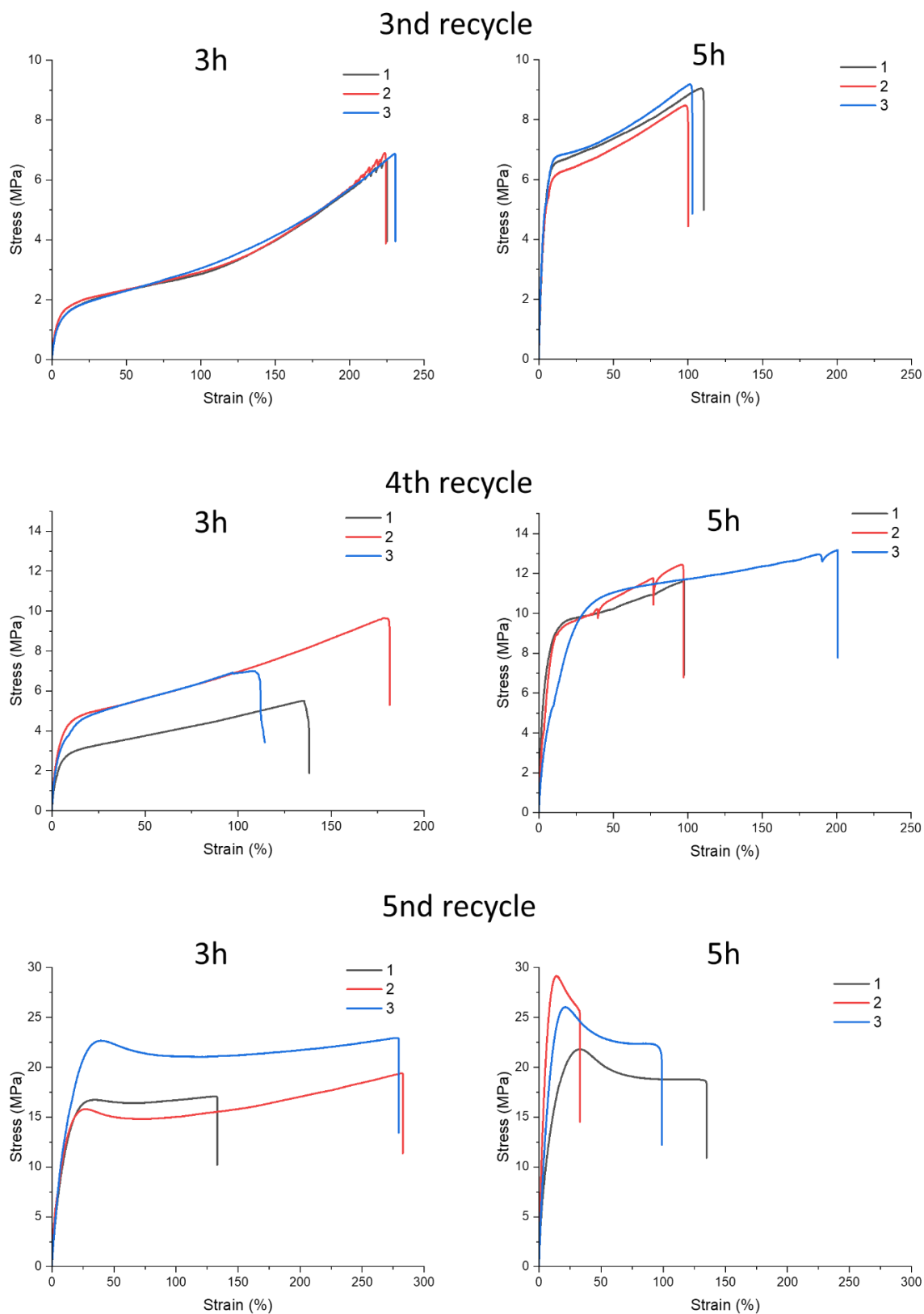
**Fig. S11.** Digital photograph of cross-cut tested SAs thermoset coated aluminum panel.

Figure S12 shows the stress-strain curves of suberic acids before recycling (which were polymerized for 4 hours and 5 hours), and after 1<sup>st</sup> and 2<sup>nd</sup> times of recycling (3 hours curing and 5 hours curing were tested).



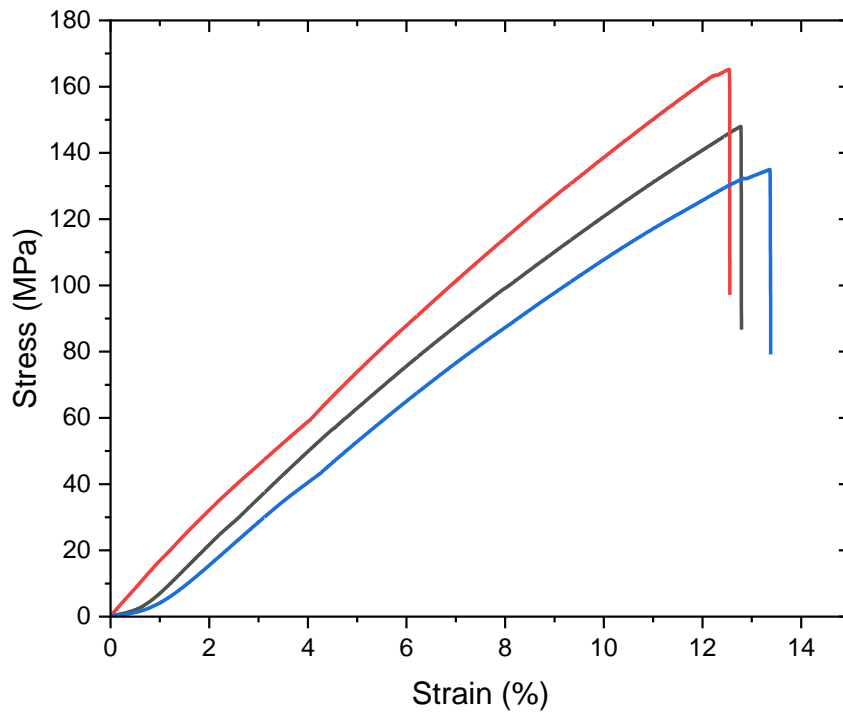
**Fig. S12.** Stress-strain curves of suberic acids thermosets before recycle, after 1<sup>st</sup> recycle and 2<sup>nd</sup> recycle. Non-recycled samples were cured for 4 or 5 hours, recycled samples were cured for 3 or 5 hours, curing temperature 190 °C.

Figure S13 shows the stress-strain curves of suberic acids after 3<sup>rd</sup>, 4<sup>th</sup>, and 5<sup>th</sup> times of recycling (3 hours curing and 5 hours curing were tested).



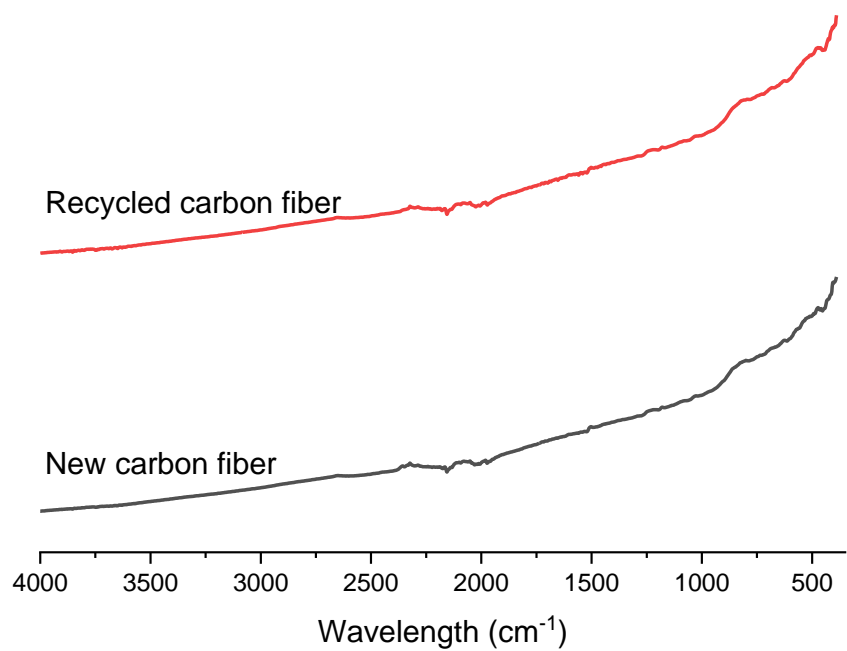
**Fig. S13.** Stress-strain curves of suberic acids thermosets after 3<sup>rd</sup>, 4<sup>th</sup>, and 5<sup>th</sup> recycle. Recycled samples were cured for 3 or 5 hours, curing temperature 190 °C.

Figure S14 shows stress-strain curves of suberinic acids/carbon fiber reinforced polymer (single ply). CFRP is prepared with 20 grams of suberinic acids and 2.5 grams of single-ply carbon fiber fabric.



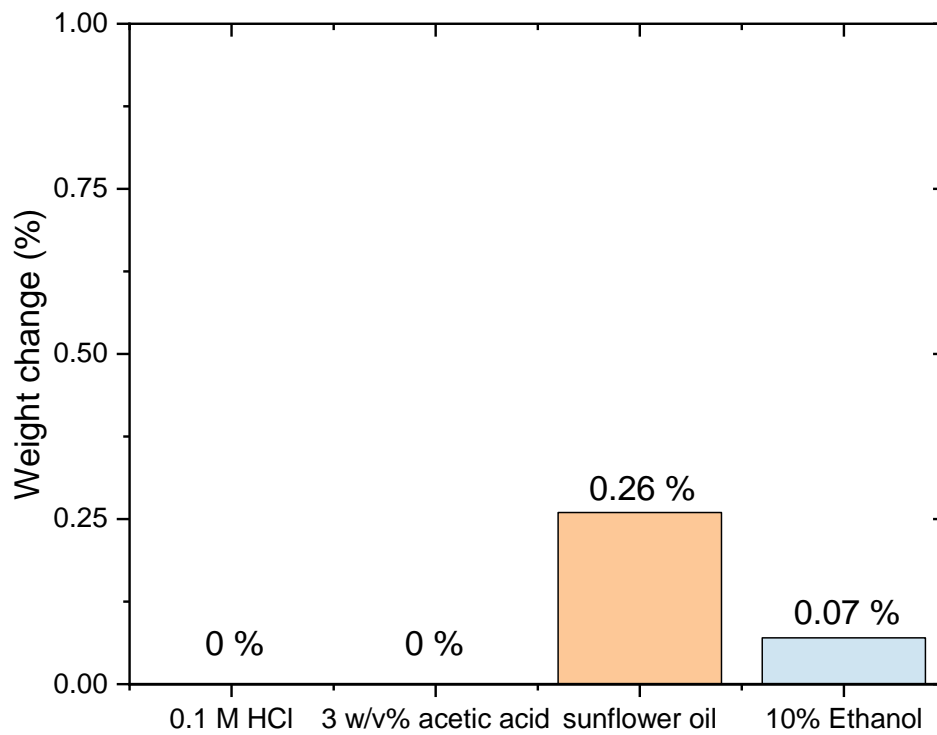
**Figure S14.** Stress-strain curves of suberinic acids/carbon fiber reinforced polymer.

Figure S15 shows the IR spectra of carbon fiber before and after the recycling process.



**Figure S15.** ATR FTIR spectra of the carbon fiber before and after the recycling process.

Figure S16 shows the weight change of suberinic acids/carbon fiber reinforced polymer after 24 hours of immersion in 0.1 M HCl solution, 3 w/v% acetic acid, sunflower oil, and 10% Ethanol. The minimal change in the weight demonstrates great stability of suberinic acids/CFRP.



**Figure S16.** Weight change of suberinic acids/carbon fiber reinforced polymer after 24 hours of immersion in 0.1 M HCl solution, 3 w/v% acetic acid, sunflower oil, and 10% Ethanol.

Table S2 shows the mechanical properties of various polymers used for comparison with the suberinic acids thermosets, where the corresponding figure is shown in Fig. 2. f).

**Table S2.** Data points used in the property comparison of suberinic acids thermosets with other biobased or synthetic thermosets in **Fig 2. f)**

	Tensile strength (MPa)	Elongation at break
Biobased polyester	3.2	200%
thermoset <sup>[2]</sup>	31	64%
Suberin-related polyester <sup>[3]</sup>	1.9	6.7%
Biobased epoxy resin <sup>[4]</sup>	7.5	28%
	22	18%
Suberin related polyester <sup>[5]</sup>	1.77	52.2%
Biobased thermoset	62.1	2.4%
polyester <sup>[6]</sup>	63.3	2.4%
	57	1.6%
Lignin epoxies thermosets <sup>[7]</sup>	5	44%
Lignin based thermoset <sup>[8]</sup>	15	10%
	7	90%
	1.3	120%
Lignin+maleic anhydride <sup>[9]</sup>	40	2.8%
Reprocesssable thermoset <sup>[10]</sup>	15	8%
Recyclable/reprocesssable thermoset <sup>[11]</sup>	22.3	402%
Recyclable/reprocesssable thermoset <sup>[11]</sup>	32.1	120%
Degradable thermoset <sup>[12]</sup>	14.5	80%
This work	1.36	373
	9.6	180
	19.4	283
	11.6	96.5
	26	98
	33	22.5

Table S3 shows the corrosion current density and inhibition efficiency of various coating systems as a comparison for the coating demonstrated in the current study.

**Table S3.** Comparison on the corrosion current density and inhibition efficiency (%) for this study and other biobased or synthetic anticorrosion coating for aluminum.

	Corrosion current density substrate (A.cm2)	Corrosion current density Coated substrate (A.cm2)	Conditions	Inhibition Efficiency (IE%)
Polydopamine based <sup>[13]</sup>	$1.49 \times 10^{-5}$	$1.8 \times 10^{-8}$	Al in 3.5 % NaCl solution	99.9%
Tannic acid based <sup>[14]</sup>	$2.6 \times 10^{-6}$	$2.2 \times 10^{-7}$	AA2024 alloy in 50 mM NaCl solution	91.5%
Lignin based <sup>[15]</sup>	$4.6 \times 10^{-8}$	$5.05 \times 10^{-10}$	Al in 5 % NaCl solution	98.9%
Lignin nanoparticle based <sup>[16]</sup>	$1.35 \times 10^{-4}$	$2.54 \times 10^{-7}$	Al in 5 % NaCl solution	99.8%
Propargylated lignin + epoxy <sup>[17]</sup>	$9.08 \times 10^{-3}$	$2.13 \times 10^{-5}$	Cu in 3.5 % NaCl solution	99.8%
Mxene + PDMS <sup>[18]</sup>	$3.5 \times 10^{-5}$	$1.49 \times 10^{-9}$	Al in 3.5 % NaCl solution	100%
Long chain fatty acids <sup>[19]</sup>	$8.18 \times 10^{-4}$	$1.48 \times 10^{-6}$	Al in 3.5 % NaCl solution	99.8%
Stearic acid based <sup>[20]</sup>	$7.26 \times 10^{-4}$	$5.01 \times 10^{-5}$	Al in 3.5 % NaCl solution	93.1%
Chitosan based <sup>[21]</sup>	$8.56 \times 10^{-6}$	$8.58 \times 10^{-8}$	Cu-Ni (90-10) alloy in 3.5 % NaCl solution	99%
Zn-eggshell particle + starch <sup>[22]</sup>	$2.105 \times 10^{-2}$	$4.392 \times 10^{-4}$	Steel in 3.5 % NaCl solution	97.9%
This study	$7.5 \times 10^{-8}$	$8.3 \times 10^{-13}$	Al in 5 % NaCl solution	100%

Table S4 shows the mean -COOH and -OH amount of initial suberinic acids, the hydrolysis product of 48 hours cured SAs thermoset, and the 5<sup>th</sup> time recycled SAs, which is quantified in mmol g<sup>-1</sup> by <sup>31</sup>P NMR spectroscopy.

**Table S4.** Mean -COOH and -OH amount in mmol g<sup>-1</sup> quantified by <sup>31</sup>P NMR spectroscopy.

	Mean -COOH amount (mmol g <sup>-1</sup> )	Mean -OH amount (mmol g <sup>-1</sup> )
Initial suberinic acids	2.05	4.24
Hydrolysis product of 48 hours cured SAs thermoset	2.39	3.9
5 <sup>th</sup> time recycled suberinic acids	2.36	5.28

### Supplementary references

- [1] J. Rizikovs, D. Godina, R. Makars, A. Paze, A. Abolins, A. Fridrihsone, K. Meile, M. Kirpluks, "Suberinic Acids as a Potential Feedstock for Polyol Synthesis: Separation and Characterization" *Polymers* **2021**, Vol. 13, Page 4380 **2021**, 13, 4380.
- [2] T. J. Lok, J. W. Wong, X. Li, Y. Fu, Y. Xue, F. H. Jamaludin, M. O. Fong, E. B. Edward, C. Ma, S. Chandren, P. S. Goh, T. W. Wong, "Biobased Itaconate Polyester Thermoset with Tunable Mechanical Properties" *Macromolecules* **2024**, 57, 2317–2328.
- [3] H. Garcia, R. Ferreira, C. Martins, A. F. Sousa, C. S. R. Freire, A. J. D. Silvestre, W. Kunz, L. P. N. Rebelo, C. Silva Pereira, "Ex situ reconstitution of the plant biopolyester suberin as a film" *Biomacromolecules* **2014**, 15, 1806–1813.
- [4] C. Menager, N. Guigo, L. Vincent, N. Sbirrazzuoli, "Suberin from Cork as a Tough Cross-Linker in Bioepoxy Resins" *ACS Appl Polym Mater* **2021**, 3, 6090–6101.
- [5] R. Perrotta, I. Kwan, V. Poliseti, M. Ek, A. J. Svagan, M. S. Hedenqvist, "Birch-Bark Suberin-Reconstructed Polyester Film as Packaging Materials" *ACS Sustain Chem Eng* **2025**, DOI 10.1021/ACSSUSCHEMENG.5C02590.
- [6] M. A. Hofmann, A. T. Shahid, M. Garrido, M. J. Ferreira, J. R. Correia, J. C. Bordado, "Biobased Thermosetting Polyester Resin for High-Performance Applications" *ACS Sustain Chem Eng* **2022**, 10, 3442–3454.
- [7] C. Gioia, G. Lo Re, M. Lawoko, L. Berglund, "Tunable Thermosetting Epoxies Based on Fractionated and Well-Characterized Lignins" *J Am Chem Soc* **2018**, 140, 4054–4061.
- [8] D. Di Francesco, D. Rigo, K. Reddy Baddigam, A. P. Mathew, N. Hedin, M. Selva, J. S. M. Samec, "A New Family of Renewable Thermosets: Kraft Lignin Poly-adipates" *ChemSusChem* **2022**, 15, e202200326.
- [9] P. Verdross, S. Guinchard, R. T. Woodward, A. Bismarck, "Black liquor-based epoxy resin: Thermosets from untreated kraft lignin" *Chemical Engineering Journal* **2023**, 475, 145787.
- [10] B. Zhang, K. Kowsari, A. Serjouei, M. L. Dunn, Q. Ge, "Reprocessable thermosets for sustainable three-dimensional printing" *Nat Commun* **2018**, 9, 1–7.
- [11] B. Qin, S. Liu, Z. Huang, L. Zeng, J. F. Xu, X. Zhang, "Closed-loop chemical recycling of cross-linked polymeric materials based on reversible amidation chemistry" *Nature Communications* **2022** 13:1 **2022**, 13, 1–9.
- [12] R. J. Dreiling, K. Huynh, B. P. Fors, "Degradable thermosets via orthogonal polymerizations of a single monomer" *Nature* **2025**, 638, 120–125.
- [13] J. Ou, J. Wang, J. Zhou, S. Liu, Y. Yu, X. Pang, S. Yang, "Construction and study on corrosion protective property of polydopamine-based 3-layer organic coatings on aluminum substrate" *Prog Org Coat* **2010**, 68, 244–247.
- [14] R. del Olmo, A. Bastos, K. Yasakau, A. Sushkova, R. Arrabal, J. Tedim, "Corrosion inhibitor from nature: Fundamentals of tannic acid inhibition for AA2024 alloy" *Appl Surf Sci* **2025**, 680, 161434.
- [15] J. Carlos De Haro, L. Magagnin, S. Turri, G. Griffini, "Lignin-Based Anticorrosion Coatings for the Protection of Aluminum Surfaces" *ACS Sustain Chem Eng* **2019**, 7, 6213–6222.

- [16] A. Moreno, J. Liu, R. Gueret, S. E. Hadi, L. Bergström, A. Slabon, M. H. Sipponen, "Unravelling the Hydration Barrier of Lignin Oleate Nanoparticles for Acid- and Base-Catalyzed Functionalization in Dispersion State" *Angewandte Chemie International Edition* **2021**, *60*, 20897–20905.
- [17] I. Pylypchuk, O. Tkachenko, T. Budnyak, M. Sipponen, "Beta-Radiation-Resistant Anticorrosion Coatings Based on Lignin" *Small Science* **2025**, DOI 10.1002/SMSC.202500007.
- [18] Y. Zhang, C. Chen, Z. Chen, T. Zhang, Y. Wang, S. Cao, J. Ma, "Superior Anticorrosion Performance of Well-Dispersed MXene-Polymer Composite Coatings Enabled by Covalent Modification and Ambient Electron-Beam Curing" *ACS Appl Mater Interfaces* **2023**, *15*, 11099–11110.
- [19] S. K. Pandit, K. Yadav, P. Chauhan, A. Kumar, "Assessing the corrosion resistance for metallic surfaces using long-chain fatty acids" *RSC Applied Interfaces* **2025**, DOI 10.1039/D5LF00125K.
- [20] L. Feng, H. Zhang, Z. Wang, Y. Liu, "Superhydrophobic aluminum alloy surface: Fabrication, structure, and corrosion resistance" *Colloids Surf A Physicochem Eng Asp* **2014**, *441*, 319–325.
- [21] G. Jena, B. Anandkumar, S. C. Vanithakumari, R. P. George, J. Philip, G. Amarendra, "Graphene oxide-chitosan-silver composite coating on Cu-Ni alloy with enhanced anticorrosive and antibacterial properties suitable for marine applications" *Prog Org Coat* **2020**, *139*, 105444.
- [22] V. S. Aigbodion, E. Dinneya-Onuoha, "Unveiling the anti-corrosion properties of Zn-eggshell particle composite coatings on mild steel in seawater-simulated solution using starch as a modifier" *RSC Adv* **2024**, *14*, 24548–24560.